Surface spin waves in antiferromagnets

B. Lüthi* and D. L. Mills
Physics Department, University of California, Irvine, California 92717

R. E. Camley
Physics Department, University of Colorado, Colorado Springs, Colorado 80907

(Received 19 April 1983)

A complete theory for dipolar antiferromagnetic surface spin waves is given. Analytic forms are derived for the dispersion relation and regions of stability. Applications to representative uniaxial antiferromagnets (MnF_2, $GdAlO_3$, FeF_2) are shown and possible experimental methods for verification are discussed. The case of exchange-dominated antiferromagnetic surface spin waves is briefly mentioned.

I. INTRODUCTION

Ferromagnetic surface spin waves have been observed in ferromagnets (Ni,Fe,EuO) and are well documented.[1] Antiferromagnetic surface spin waves (ASSW) on the other hand have not been observed so far. We distinguish between dipolar ASSW and exchange-type ASSW. The dipolar ASSW exist for long-wavelength excitations where the macroscopic dipolar fields set up by the precessing magnetic moments on each sublattice provide a significant contribution to the excitation energy of the spin wave. They are the antiferromagnetic analog of the Damon-Eshbach modes for ferromagnets. The exchange-type ASSW have been discussed theoretically in a microscopic way,[2,3] and we shall comment on these excitations briefly.

It is now well established that dipolar contributions have a measurable effect on antiferromagnetic resonance spectra in uniaxial antiferromagnets. The modified spin-wave spectra have been calculated in the continuum limit[4] and magnetostatic modes have been observed in MnF_2.[5] Calculations also exist for the long-wavelength surface magnetostatic mode spectra for antiferromagnets.[6,7] The purpose of the present communication is to correct some inconsistencies in these papers, to give symmetry arguments for these ASSW modes, and to give numerical calculations for typical uniaxial antiferromagnets (MnF_2, $GdAlO_3$, and FeF_2). On the basis of these applications we shall comment on the possibility of observing these modes and the related exchange-type surface modes. In the following section we develop the theory and give the necessary formulas for the excitation frequency, the stability conditions, and a symmetry argument. Afterwards we give numerical applications and a discussion.

II. THEORY

The analysis given here closely follows Refs. 6 and 8. Let the easy axis be the z direction and the sublattices be denoted by A,B. Then $M_{T_i}=M_{A_i}+M_{B_i}$ with $i=x,y$. $M_{T_x}=\chi_{xx}h_x+i\chi_{xy}h_y$, $M_{T_y}=-i\chi_{xy}h_x+\chi_{yy}h_y$, where the susceptibility tensor χ_{ij} reads

$$\chi_{xx}=\chi_{yy}=\chi_+ +\chi_-,\quad \chi_{xy}=-\chi_{yx}=\chi_+ -\chi_- , \tag{1}$$

with

$$\chi_\pm=\frac{\gamma^2 H_a M}{\Omega^2-(\omega\pm\gamma H_0)^2} .$$

Here $(\Omega/\gamma)^2=2H_{ex}H_a+H_a^2$, where H_a is the anisotropy field, H_{ex} is the exchange field,[9] H_0 is the applied field, M is the saturation magnetization of one of the sublattices, and γ is the gyromagnetic ratio (negative number). Here Ω is the antiferromagnetic resonance frequency in the zero applied field, and $\Omega/|\gamma|$ is the field where bulk antiferromagnetic spin waves soften, and enter the spin-flop state, which we shall discuss briefly below.

For magnetostatic modes we have the dipolar equations $\mathrm{curl}\,\vec{h}_d=0$, $\mathrm{div}\,\vec{b}=0$, where $\vec{h}_d$ is the macroscopic fluctuating dipolar field, and $b_i=h_{d_i}+4\pi M_{T_i}$. With $\vec{h}_d=-\mathrm{grad}\phi$, one obtains the Walker equation[8]

$$(1+4\pi\chi_{xx})\left[\frac{\partial^2\phi}{\partial x^2}+\frac{\partial^2\phi}{\partial y^2}\right]+\frac{\partial^2\phi}{\partial z^2}=0 . \tag{2}$$

For bulk spin waves we make the ansatz $\phi_b=\phi_0 e^{i\vec{q}\cdot\vec{x}}$. Insertion of this relation and χ_{xx} from Eq. (1) gives the bulk dispersion relation[4]

$$\left[\frac{\omega_b}{\gamma}\right]^2=\left[\frac{\Omega}{\gamma}\right]^2+H_0^2+4\pi M H_a\cos^2\theta \pm 2\left[H_0^2\left[\frac{\Omega}{\gamma}\right]^2+4\pi M H_a H_0^2\cos^2\theta+4\pi^2M^2H_a^2\cos^4\theta\right]^{1/2} . \tag{3}$$

Here $\pi/2-\theta$ is the angle between the z axis along which the Zeeman field H_0 is directed and the propagation direction $\vec{q}$.

Now we turn to the ASSW. We take as the surface the $y=0$ plane and fix the direction of propagation along the surface plane by the wave vector $\vec{q}_{||}$, which makes an angle θ with the x direction [see inset of Fig. (1a)]. At the end of this section we shall comment on the configuration with H_0 normal to the plane. For $y>0$ (inside the medium) we make the ansatz for the magnetic scalar potential

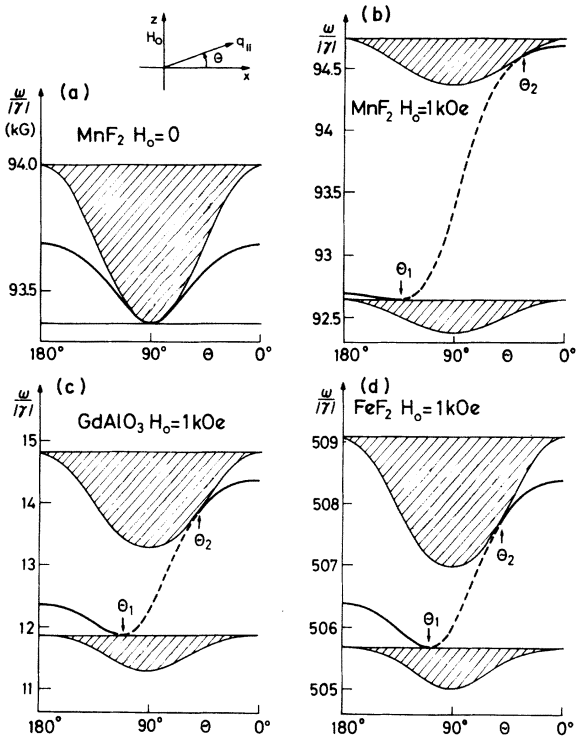

FIG. 1. Frequency of bulk and dipolar surface spin waves as a function of angle of propagation for various materials and fields. Arrows indicate points (θ_1,θ_2), where bulk and surface spin-wave frequencies touch. Inset in (a) indicates geometrical arrangement of $\vec{H}_0,\vec{q}_{||}$.

$$\phi=\phi_0 e^{i\vec{q}_{||}\cdot\vec{x}-\alpha y},$$

and by using Eq. (2) we obtain

$$\alpha^2=q_{||}^2\left[\cos^2\theta+\frac{\sin^2\theta}{1+4\pi\chi_{xx}}\right]. \tag{4a}$$

For $y<0$ (outside the material) $\nabla^2\phi=0$ holds, and with the boundary continuity conditions for the tangential components of $\vec{h}_d$ and the y component of $\vec{b}$, we obtain

$$\alpha=-\frac{q_{||}}{1+4\pi\chi_{xx}}(1-4\pi\chi_{xy}\cos\theta)\,. \tag{4b}$$

By eliminating α from (4a), (4b) gives

$$\chi_{xx}[1+\cos^2\theta(1+4\pi\chi_{xx})]=-2\chi_{xy}\cos\theta[1-2\pi\chi_{xy}\cos\theta]\,, \tag{5}$$

and with χ_{ij} inserted, we obtain the equation for the ASSW:

$$\frac{\omega_s}{\gamma}=-\frac{2H_0\cos\theta}{1+\cos^2\theta}\pm\left[\left[\frac{\Omega}{\gamma}\right]^2-\frac{H_0^2\sin^4\theta}{(1+\cos^2\theta)^2}+\frac{8\pi MH_a\cos^2\theta}{1+\cos^2\theta}\right]^{1/2}. \tag{6}$$

Taking $q_x=q_{||}\cos\theta$, we notice that the two solutions of Eq. (6), $(\omega_{s_1}/\gamma)(\theta)$ for the positive sign, and $(\omega_{s_2}/\gamma)(\theta)$ for the negative sign, are related by

$$\frac{\omega_{s_1}(\theta)}{\gamma}=-\frac{\omega_{s_2}(\pi-\theta)}{\gamma}\,.$$

If we choose $\omega_s/|\gamma|$ to be positive for $H_0=0$, we take the $-$ sign in Eq. (6) and obtain

$$\frac{\omega_s}{|\gamma|}=\frac{2H_0\cos\theta}{1+\cos^2\theta}+\left[\left[\frac{\Omega}{\gamma}\right]^2-\frac{H_0^2\sin^4\theta}{(1+\cos^2\theta)^2}+\frac{8\pi MH_a\cos^2\theta}{1+\cos^2\theta}\right]^{1/2}. \tag{7}$$

Illustrative examples for $\omega_s/|\gamma|$ and $\omega_b/|\gamma|$ are given in Fig. 1 as a function of angle θ. The bulk bands in Fig. 1 arise from the fact that we specify in this figure only the propagation direction parallel to the surface. For bulk modes there also exist many different allowed values for the wave vector perpendicular to the surface, and this leads to a band of allowed frequencies. Turning to the surface modes we see nonreciprocal features characteristic of magnetostatic surface waves,[1,10–12] i.e., $\omega(+\vec{q}_{||})\neq\omega(-\vec{q}_{||})$. In addition we notice that the ASSW do not penetrate the bulk spin-wave continuum, but they merely touch it at a critical angle $\theta_{1,2}$. This is exactly analogous to the case of Damon-Eshbach magnetostatic modes for ferromagnets.[8] This fact was not explicitly recognized in an earlier treatment.[7]

Next we investigate the stability of these ASSW. The condition is given by $\alpha>0$, i.e.,

$$\alpha=-q_{||}\frac{[1-4\pi\cos\theta(\chi_+-\chi_-)]}{1+4\pi(\chi_++\chi_-)}>0\,.$$

This condition ensures that the amplitude of the wave decays exponentially as it moves away from the surface. This leads to stability regions for ASSW in direct analogy to the case of ferromagnetic Damon-Eshbach modes. By putting in the expression for $\chi_\pm$ we can again use the symmetry argument above:

$$\alpha=-q_{||}\frac{\left[\left[\frac{\Omega}{\gamma}\right]^2-\left[\frac{\omega}{\gamma}+H_0\right]^2\right]\left[\left[\frac{\Omega}{\gamma}\right]^2-\left[\frac{\omega}{\gamma}-H_0\right]^2\right]-16\pi MH_a\cos\theta\left[\frac{\omega}{\gamma}H_0\right]}{\left[\left[\frac{\Omega}{\gamma}\right]^2-\left[\frac{\omega}{\gamma}+H_0\right]^2\right]\left[\left[\frac{\Omega}{\gamma}\right]^2-\left[\frac{\omega}{\gamma}-H_0\right]^2\right]+8\pi MH_a\left[\left[\frac{\Omega}{\gamma}\right]^2-\left[\frac{\omega}{\gamma}\right]^2-H_0^2\right]}>0\,. \tag{8}$$

From Eq. (8) it is evident that if the stability condition is fulfilled for $(\omega_{s_1}/\gamma)(\theta)$, for example, then it is also fullfilled for $(\omega_{s_2}/\gamma)(\pi-\theta)$, since the only term displaying nonreciprocal features in Eq. (8) is the second term in the numerator and

$$\cos\theta\frac{\omega_{s_1}(\theta)}{\gamma}=\cos(\pi-\theta)\frac{\omega_{s_2}(\pi-\theta)}{\gamma}\ .$$

Therefore both solutions and their stability regions are the same, except if one solution is for q_x, the other one is for $-q_x$. In other words, the wave-type solution $(q_x x-\omega_s t)$ changes to $-(q_x x-\omega_s t)$, and the two solutions are thus identical in physical content. These stability criteria were used properly but not mentioned[7] or not given correctly[6] in previous work.

The decay constant α determines the penetration depth of the surface spin wave. It can be calculated from Eq. (8). It is seen that α is proportional to the magnitude of the wave vector $q_{||}$. The surface spin-wave frequency, on the other hand, is only dependent on the propagation direction, as long as the frequency is in the magnetostatic region. The value of $q_{||}$ is determined by the experiment (surface acoustic wave vector for the magnetoelastic crossover in the case of magnon-phonon resonance or the momentum transfer in the case of Brillouin scattering).

For $H_0>\Omega/|\gamma|$, i.e., in the spin-flop state where the spins are canted, one has ferromagneticlike susceptibilities. The surface and bulk spin waves have ferromagneticlike character. Since they are no longer true ASSW we shall not pursue this point any further here, but we will give only the formulas for bulk spin waves and surface spin waves[13] (for propagation direction along the x axis). The following is the formula for bulk waves:

$$\left[\frac{\omega}{\gamma}\right]^2=2H_{\rm ex}(H_0\cos\theta+H_a\cos2\theta)+16\pi MH_{\rm ex}\cos^2\theta\left[\frac{q_x}{q}\right]^2+8\pi M(H_0\cos\theta+H_a\cos2\theta)\left[\frac{q_y}{q}\right]^2 . \quad (9)$$

The following is the formula for surface waves:

$$\left[\frac{\omega_s}{|\gamma|}\right]_x=(H_{\rm ex}+4\pi M)\cos\theta+\frac{H_0\cos\theta+H_a\cos2\theta}{2\cos\theta}\ .$$

Here

$$\cos\theta=\frac{H_0}{2H_{\rm ex}-H_a}$$

determines the canting angle of the sublattices. The stability region for the spin-flop state is

$$H_2=\left[\frac{2H_{\rm ex}-H_a}{2H_{\rm ex}+H_a}\right](2H_{\rm ex}H_a+H_a^2)^{1/2}$$

$$<H_0<2H_{\rm ex}-H_a=H_3\ .$$

In Fig. 6 we show bulk and surface spin waves for the antiferromagnetic state, the spin-flop state, and the paramagnetic state. The calculations are made for the values of $GdAlO_3$. As in the ferromagnetic case the surface spin waves in the spin-flop region exhibit strong nonreciprocal behavior.[13]

While the geometry discussed above is the most interesting one for nonreciprocal features or for experimental observation, there are other possible configurations.[6] We only mention that for the easy axis and for H_0 being perpendicular to the surface, there do not exist stable ASSW if only dipolar interactions are included, again a result identical to the ferromagnet.[10]

III. NUMERICAL RESULTS FOR UNIAXIAL ANTIFERROMAGNETS

We would like to apply the results derived above to typical cases which might be checked experimentally. We give results for three antiferromagnets which are well characterized and sufficiently different in their physical parameters so that they exhibit features which might be detectable using low-frequency ultrasonics,[14] microwave techniques,[5] Brillouin scattering,[1] or by far-infrared experiments. In Table I we list physical properties of MnF_2,[15] $GdAlO_3$,[16] and FeF_2.[17] All these substances can be classified as uniaxial antiferromagnets. For $GdAlO_3$ with its orthorhombic crystal structure there are some small differences from uniaxial behavior[16] which we neglect for our purposes. $GdAlO_3$ has an easily accessible antiferromagnetic resonance and spin-flop field of $\sim$12 kOe; MnF_2 has a spin-flop field of 93 kOe, still accessible with superconducting magnets; and for FeF_2 with a spin-flop field of 506 kOe, infrared techniques are called for.

For completeness sake we show in Fig. 1(a) bulk and surface spin waves for $H_0=0$ for MnF_2. The ASSW are stable in the whole region. In Figs. 1(b)–1(d) we give corresponding results for a small applied field of $H_0=1$ kOe. We notice that the critical angles $\theta_{1,2}$, which for $H_0=0$ are at $\theta=\pi/2$ split to $\theta_{1,2}\neq\pi/2$. The ASSW spectrum does not intersect the bulk spin-wave band but touches it at these two points. The stable region for ASSW is then between $\pi-\theta_1$ and θ_2-0 (solid lines in Fig. 1), and the unstable region is between θ_1 and θ_2, $\pi/2$ included (dotted lines). Notice the strong analogy to Damon-Eshbach modes for the ferromagnetic case. Also notice that the

TABLE I. Physical properties of $GdAlO_3$, MnF_2, and FeF_2.

	$GdAlO_3$	MnF_2	FeF_2
Néel temperature T_N (K)	3.87	67	79
Exchange field $H_{\rm ex}$ (T)	1.88	55	54
Anisotropy field H_a (T)	0.365	0.787	20
Sublattice magnetization M (G)	624	600	560
Spin-flop field Ω/γ (T)	1.226	9.337	50.6

maximum splitting between bulk waves and ASSW is for $\theta=\pi$ about 50 Oe for MnF_2, about 500 Oe for $GdAlO_3$, and about 350 Oe for FeF_2. These are rather small splittings for optical measurements. Therefore we present results for higher fields close to the spin-flop transition.

In Figs. 2 and 3 we present stability curves for ASSW as a function of applied fields for MnF_2 and $GdAlO_3$, the case of FeF_2 being quite similar. The lower branch belongs to the angular region $\pi-\theta_1$ and the higher branch to θ_2-0. The regions of stability are found from Eq. (8). As seen from these figures the branches are quite narrow, becoming even narrower in the intermediate-field region. But near $H_0=\Omega/|\gamma|$ the region of stability expands again. These stability regions are somewhat different from the stability regions given in Ref. 6.

In Fig. 4 we show bulk and surface spin waves for MnF_2 for $H_0=93$ kOe, 370 Oe below the spin-flop transition. In Fig. 4 we concentrate on the lower branch where $\omega_b/|\gamma|=615$ Oe and $\omega_s/|\gamma|=692$ Oe for $\theta=\pi$. Such a splitting can be detected in principle by Brillouin scattering spectroscopy, but the spin-flop transition is not very sharp.[14]

The case of $GdAlO_3$ is more advantageous. For $H_0=12$ kOe, i.e., 260 Oe below $\Omega/|\gamma|$ the resulting spin-wave spectra are shown in Fig. 5. We notice, for example, for the $\theta=\pi$ geometry a bulk spin wave at 803 Oe (16 Gc) and a ASSW at 1420 Oe (28.4 Gc). Such modes could be detected by Brillouin scattering techniques. In addition an applied field of 12 kOe can be generated by electromagnets. Figures 5 and 6 demonstrate that the ASSW could be observed either by Brillouin scattering or by microwave techniques. Figure 6 shows the antiferromagnetic state and the spin-flop state for $GdAlO_3$ with spin-wave propagation along q_x. The spin-flop region $H_2<H_0<H_3$ and the paramagnetic region $H>H_3$ will be discussed in greater detail elsewhere.[13]

In the case of FeF_2 a higher magnetic field does not help because we had to use inaccessible fields to bring the spin-wave spectra down to about the microwave region. If we apply a 100 kOe field, the splitting of the bulk spin wave and the ASSW is only 12 Oe compared to 350 Oe for 1 kOe. We conclude that dipolar surface spin waves are rather difficult to observe in materials with a large energy gap such as FeF_2. The most promising case seems to be $GdAlO_3$, as discussed above. Brillouin scattering or microwave experiments should enable one to observe ASSW. Magnetoelastic interaction with ultrasound[14] still proves to be difficult because we had to move too close to the spin-flop transition which always was somewhat smeared out.

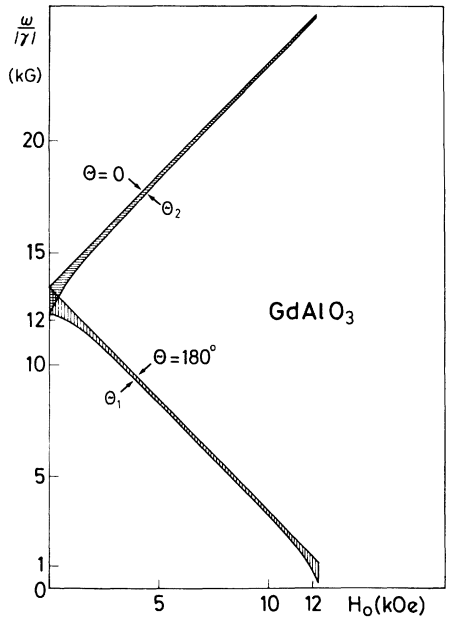

FIG. 3. Region of stability for ASSW as a function of applied field for $GdAlO_3$.

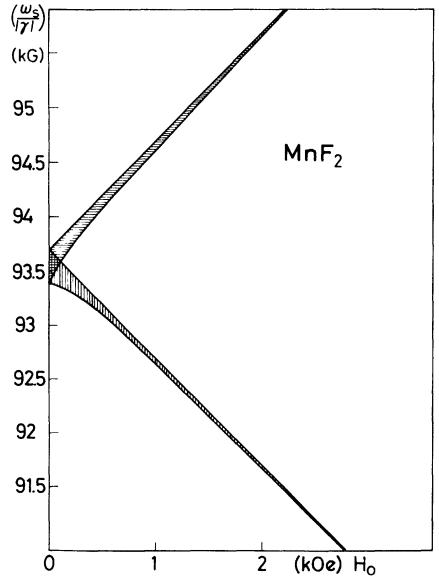

FIG. 2. Region of stability for ASSW as a function of applied field for MnF_2.

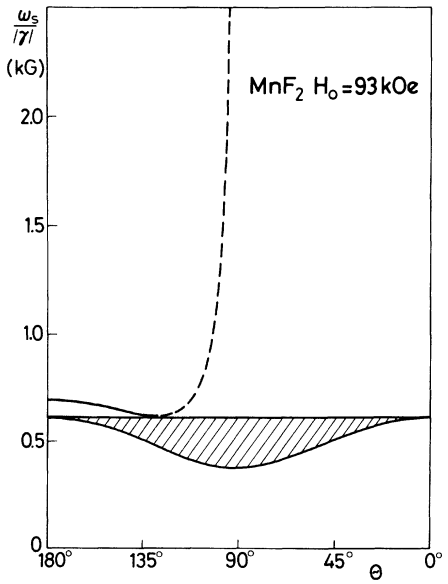

FIG. 4. Frequency of ASSW near spin-flop field (lower branch) in MnF_2.

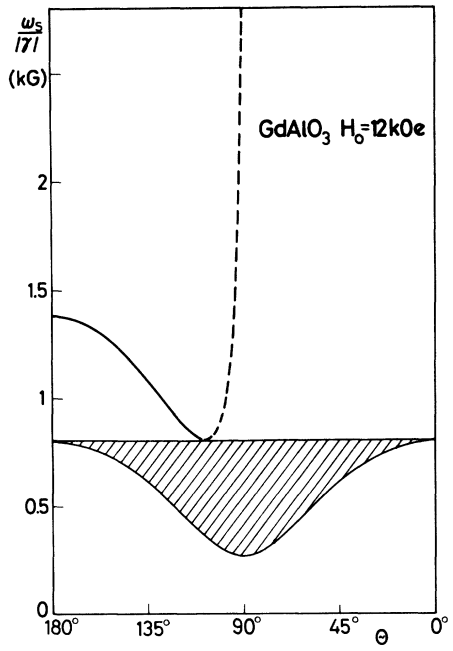

FIG. 5. Frequency of ASSW near spin-flop field (lower branch) in $GdAlO_3$.

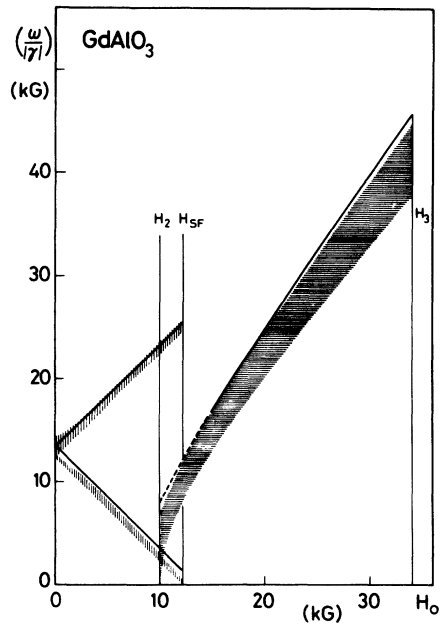

FIG. 6. Bulk spin waves (shaded area) and surface spin waves (in the x direction) for the antiferromagnetic region $H < H_{SF}$ (where H_{SF} represents the spin-flop field) and the spin-flop region $H_2 < H_0 < H_3$ for $GdAlO_3$.

Finally we would like to comment on exchange-type surface spin waves. These are modes which can best be studied with H_0 parallel to the easy axis, and the easy axis preferably normal to the surface. Notice that the dipolar ASSW described above are unstable for this configuration. It has been shown theoretically that there exists a surface spin-flop field[2,3]

$$\frac{\Omega_1}{\gamma} = \frac{1}{\sqrt{2}} \frac{\Omega}{\gamma}$$

and that for $H_0 > \Omega_1/\gamma$, the flopped state increases in size proportional to $(\Omega/\gamma - H_0)^{-1}$. However, for actual fields rather close to Ω/γ, the volume involved is still rather small[15] ($\lesssim 100$ atomic layers). We conclude that it is extremely difficult to observe these exchange-dominated surface spin waves.

ACKNOWLEDGMENTS

We would like to thank J. P. Kotthaus for bringing Refs. 6 and 15 to our attention and for informative discussions. One of us (B.L.) would like to thank the members of the Solid State Physics Group at the University of California at Irvine for their warm hospitality.

*Permanent address: Physikalisches Institut, Universität Frankfurt, D-6000 Frankfurt am Main 1, Germany.

[1]P. Grünberg and F. Metawe, Phys. Rev. Lett. 39, 1561 (1977); J. R. Sandercock and W. Wettling, J. Appl. Phys. 50, 7784 (1979) and references contained in it.
[2]D. L. Mills, Phys. Rev. Lett. 20, 18 (1968).
[3]F. Keffer, H. Chow, Phys. Rev. Lett. 31, 1061 (1973).
[4]R. Loudon and P. Pincus, Phys. Rev. B 132, 673 (1963).
[5]J. P. Kotthaus and V. Jaccarino, Phys. Rev. Lett. 28, 1649 (1972) and references contained in it.
[6]V. V. Tarasenko and V. D. Kharitonov, Zh. Eksp. Teor. Fiz. 60, 2321 (1971) [Sov. Phys.—JETP 33, 1246 (1971)].
[7]R. E. Camley, Phys. Rev. Lett. 45, 283 (1980).
[8]D. L. Mills in *Surface Excitations,* edited by V. M. Agranovich and R. Loudon (North-Holland, Amsterdam, 1983), Chap. 3.
[9]The exchange field used here is a combination of the true exchange field and the Lorentz field of one sublattice acting on the other. That is H_{ex} (this paper)$=H_{ex}-4\pi M/3$. For a detailed discussion of this point, see R. M. White, J. Appl. Phys. 36, 3653 (1965); A. Brooks Harris, Phys. Rev. 143, 353 (1966).
[10]Talat S. Rahman and D. L. Mills, J. Appl. Phys. 53, 2084 (1982).
[11]R. L. Scott and D. L. Mills, Phys. Rev. B 15, 3545 (1977).
[12]J. Heil, B. Lüthi, and P. Thalmeier, Phys. Rev. B 25, 6515 (1982).
[13]B. Lüthi and R. Hock (unpublished).
[14]C. Lingner and B. Lüthi, J. Appl. Phys. 53, 8061 (1982).
[15]S. P. Vernon, R. W. Sanders, and A. R. King, Phys. Rev. B 17, 1460 (1978).
[16]K. W. Blazey, H. Rohrer, and R. Webster, Phys. Rev. B 4, 2287 (1971).
[17]R. C. Ohlmann and M. Tinkham, Phys. Rev. 123, 425 (1961).